ADVANCED MATERIALS
www.advmat.de

www.MaterialsViews.com

Buckled Germanene Formation on Pt(111)

Linfei Li, Shuang-zan Lu, Jinbo Pan, Zhihui Qin, Yu-qi Wang, Yeliang Wang,* Geng-yu Cao, Shixuan Du, and Hong-Jun Gao**

Due to its novel properties and potential applications, graphene has been attracting remarkable attention worldwide in science and technology.[1–7] The tremendous progress in graphene research has motivated us to investigate analogous 2D crystalline systems—new two-dimensionally ordered and layered materials composed of elements other than carbon. For example, silicene, the silicon equivalent of graphene, has recently attracted attention, both in theoretical and experimental fields.[8–12] Moreover, there has been considerable interest in the hypothetical germanium analogue of graphene called "germanene"—a one-atom-thick germanium layer with a honeycomb structure. Theoretical models of free-standing single-layer germanium have been studied. For instance, based on theoretical calculations, Cahangirov et al. proposed that germanium atoms would prefer to form a corrugated sheet structure.[8] In particular, a quantum-spin Hall effect is predicted in buckled germanene,[13] and high-T_c superconductivity is anticipated in doped germanene (where T_c represents the critical temperature for superconductivity).[14] Thus, the developing methods for germanene growth is certainly of great importance; however, to the best of our knowledge, the actual fabrication of germanene has not yet been reported.

In this Communication, we report on the fabrication of graphene-like germanene sheet on a Pt(111) surface. The choice of a Pt(111) substrate is based on several advantageous characteristics of Pt(111), such as its hexagonal symmetry serving as a growth template and its weaker interfacial interaction with adsorbed 2D honeycomb sheets (e.g., graphene) relative to other metals.[15–17] Germanium was firstly deposited onto a Pt(111) surface, and after annealing, a distinct well-ordered superstructure was obtained. The structure was characterized as a ($\sqrt{19} \times \sqrt{19}$) superstructure with respect to the substrate lattice by low-energy electron diffraction (LEED) and scanning tunneling microscopy (STM). Moreover, our density functional theory (DFT)-based ab initio calculations revealed a honeycomb structure of germanium with 2D continuity on the Pt(111) substrate. Considering our experimental observations together with the calculations, we conclude that the germanene fabricated on this surface was a 2D continuous layer with a buckled conformation.

The structure of the germanium layer formed on the Pt(111) surface, characterized macroscopically by LEED, is shown in **Figure 1**a. The six outer symmetric bright spots can be assigned to the pristine Pt(111) substrate, which has six-fold symmetry. The additional distinct diffraction spots originate from the germanium superstructures. For clarity, we sketched a map of the diffraction spots of the superstructure in reciprocal space (Figure 1b), where the reciprocal vectors of each group of spots are indicated by differently colored arrows. Aside from the (1×1) diffraction spots of the Pt(111) lattice, two symmetrically equivalent domains exist, identified by red and blue spots, respectively. Aiming to understand this LEED pattern more thoroughly, a schematic diagram in real space consistent with the diffraction patterns is provided in Figure 1c. This diagram directly reveals the commensurable relation between the germanium adlayer and the substrate lattice. Germanium forms a superstructure with matrix $\begin{bmatrix} 2 & -3 \\ 3 & 5 \end{bmatrix}$ or the equivalent $\begin{bmatrix} 3 & -2 \\ 2 & 5 \end{bmatrix}$, and the corresponding angles between the close-packed direction of Pt[$1\bar{1}0$] and this superstructure can be obtained as 36.6° and 23.4°, respectively. From the data, this superstructure can be easily identified as a ($\sqrt{19} \times \sqrt{19}$) superstructure with respect to the Pt(111) substrate.

In order to characterize the germanium adlayer in detail, we subsequently carried out STM measurements. The large-scale STM image in **Figure 2**a shows the long-range order of the germanium superstructure formed on the Pt(111) surface. One of the supercells is marked by the black rhombus. The orientation of the supercell is rotated about 23° relative to Pt[$1\bar{1}0$] direction. The corresponding high-resolution STM image of the germanium adlayer is displayed in Figure 2b, demonstrating two other protrusions with different image contrast inside each supercell. Figure 2c shows the line profile along the dashed line of Figure 2b, revealing that the periodicity of the brightest protrusions in the STM image is about 1.2 nm. This distance is equal to the dimension of ($\sqrt{19} \times \sqrt{19}$) superlattice of the Pt(111) surface; the lattice constant of Pt(111) is 0.277 nm ($\sqrt{19} \times 0.277$ nm = 1.21 nm). It is readily apparent that both the orientation and the periodicity of the germanium superstructure detected by STM are in good agreement with the analysis of the LEED pattern, confirming that a ($\sqrt{19} \times \sqrt{19}$) germanium superstructure was formed on the surface. In addition, the profile reveals a corrugation of around 0.6 Å in the germanium adlayer,

L. Li,[+] J. Pan,[+] Y.-Q. Wang, Prof. Y. Wang, Prof. S. Du, Prof. H.-J. Gao
Beijing National Laboratory of Condensed Matter Physics
Institute of Physics
Chinese Academy of Sciences
Beijing 100190, PR China
E-mail: ylwang@iphy.ac.cn; hjgao@iphy.ac.cn
S.-Z. Lu,[+] Prof. Z. Qin, Prof. G.-Y. Cao
State Key Laboratory of Magnetic Resonance and Atomic and Molecular Physics
Wuhan Institute of Physics and Mathematics
Chinese Academy of Sciences
Wuhan 430071, China
E-mail: zhqin@wipm.ac.cn
[+]These authors contributed equally to this work

DOI: 10.1002/adma.201400909

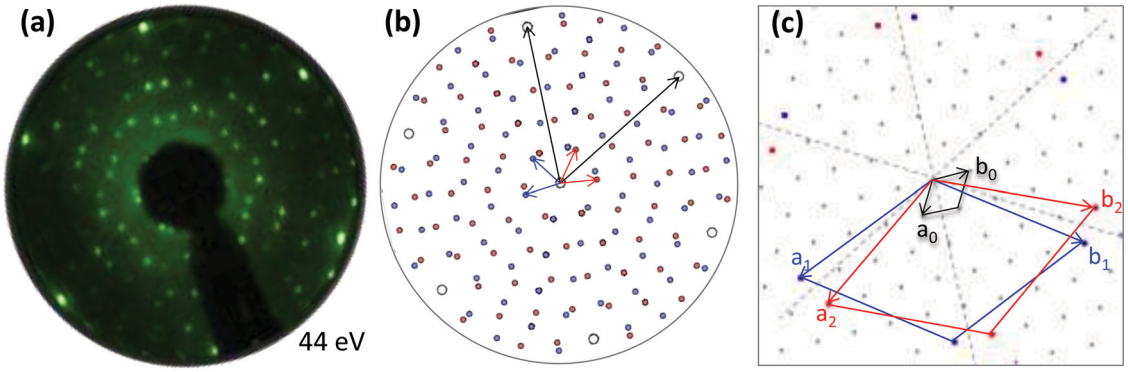

Figure 1. LEED patterns and the corresponding schematic diagram of the germanium superstructure formed on the Pt(111) surface. a) The six outer and brightest spots originate from the six-fold symmetry of the Pt(111) substrate. The additional diffraction spots are ascribed to the germanium adlayer. b) Schematic representation of the diffraction spots shown in (a), where the reciprocal vectors of each group of spots are indicated by black, red, or blue arrows. c) Schematic diagram of the diffraction spots in real space. These data reveal a ($\sqrt{19} \times \sqrt{19}$) superstructure of the germanium layer [lattice vectors (a_1, b_1) or (a_2, b_2)] with respect to the Pt(111) lattice [lattice vectors (a_0, b_0)].

indicating that different germanium atoms in the adlayer have different apparent heights with respect to the underlying Pt lattice, which we further analyzed using DFT calculations. This corrugation value is close to the buckled height (around 0.64 Å) of free-standing germanene in vacuum[8] and comparable to that of silicene on Ag(111) (0.75 Å).[9] It implies that the Ge–Pt interaction is similar to the moderate Si–Ag interaction, which facilitates the formation of silicene on Ag(111).[18]

Although Figure 2b is not an STM image at atomic resolution, it is useful for one to construct an atomic model of the germanium adlayer. Note that the lattice constant of low-buckled free-standing germanene is about 3.97–4.02 Å based on the predictions of previous theoretical studies.[8,13] In that case, the lattice constant of the (3 × 3) superlattice of the germanene is about 11.91–12.06 Å. This value is close to the periodicity of our observed structure (12 Å), the ($\sqrt{19} \times \sqrt{19}$) germanium superstructure on Pt(111). Thus, we propose the following model to account for our observations: a single-layer germanene sheet is adsorbed on the Pt(111) surface at a certain rotation angle. As the rotation angle between the close-packed direction of Pt[$1\bar{1}0$] and the ($\sqrt{19} \times \sqrt{19}$) germanium superstructure is determined to be about 23° (Figure 2a), and the angle between the direction of the (1 × 1) lattice of germanene and the direction of its (3 × 3) superlattice is 0°, we can deduce the rotation angle of the high-symmetry direction of the germanium adlayer with respect to the substrate lattice; that is, about 23° between the (1 × 1) lattice of germanene and the Pt[$1\bar{1}0$] direction. In this model, the ($\sqrt{19} \times \sqrt{19}$) supercell of the Pt(111) substrate nearly matches the (3 × 3) superlattice of the germanene sheet.

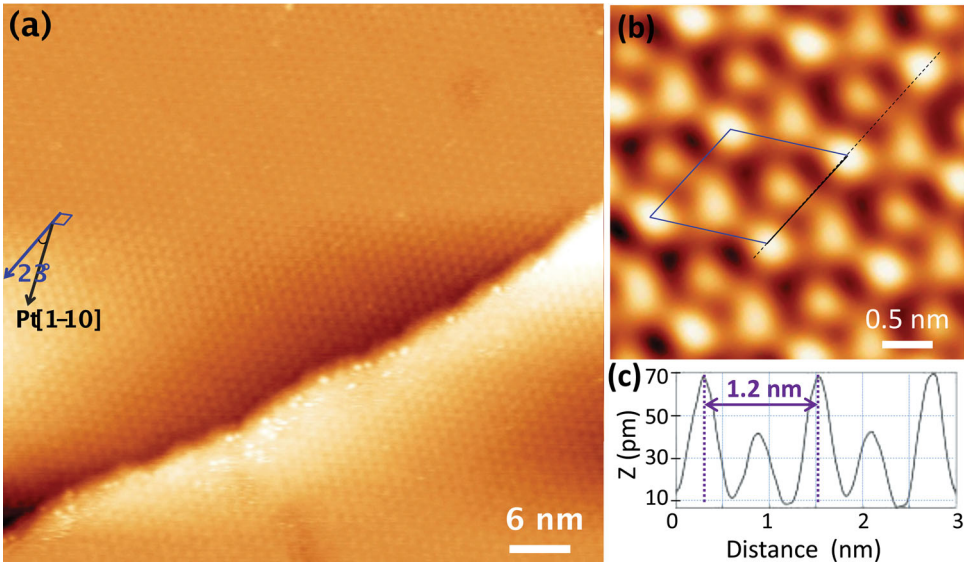

Figure 2. a) Occupied-state STM image (potential: $U = -1.45$ V, current: $I = 0.25$ nA), showing a ($\sqrt{19} \times \sqrt{19}$) superstructure of the germanium adlayer formed on the Pt(111) surface. The direction of this reconstruction is indicated by the blue arrow. The close-packed direction Pt[$1\bar{1}0$] is indicated by the black arrow. The angle between the blue and black arrows is about 23°. b) Zoomed-in STM image ($U = 1$ V, $I = 0.05$ nA) of the germanium adlayer. c) Line profile along the dashed line in (b), revealing the periodicity of the germanium superstructure (1.2 nm).

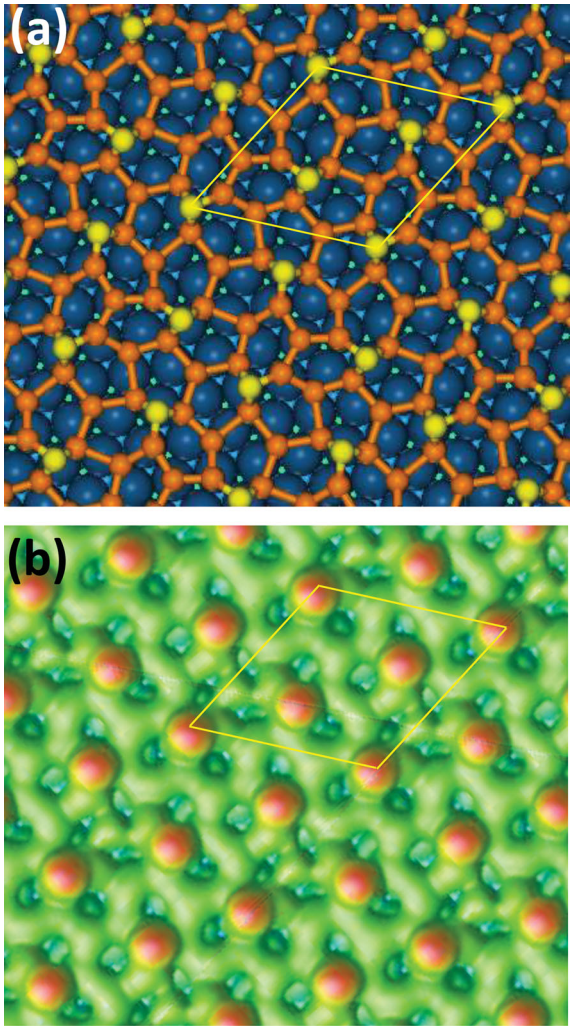

Figure 3. a) Top view of the relaxed atomic model of the (3 × 3) germanene/(√19 × √19) Pt(111) configuration. The blue, yellow, and orange spheres represent Pt, protruding Ge, and other Ge atoms, respectively; a unit cell is outlined in yellow. b) Simulated STM image, showing features identical with the experimental results. The brightness scale is represented by red > white > dark green, and a unit cell is outlined in yellow.

In order to obtain a detailed structural analysis of the germanium adlayer on Pt(111) and a deep understanding of the germanene/Pt(111) system, we calculated the geometric and electronic structures using DFT-based ab initio calculations, and we performed the corresponding STM simulations using the Tersoff–Hamann approach.[19] Several models (different locations for the germanium atoms with respect to the substrate) were calculated. It turns out that the model with a honeycomb structure (germanene) shown in **Figure 3**a (top view) is the most stable configuration. The binding energy of this configuration is about −1.39 eV per germanium atom. There are 18 germanium atoms per (√19 × √19) unit cell (the yellow rhombus). Different germanium atoms are situated in different chemical environments with respect to the Pt(111) surface. Such differences could account for the overall configuration of the germanene layer.

The simulated STM image is shown in Figure 3b, and one unit cell is indicated as a yellow rhombus. There are four protrusions at the vertices of the rhombus and two at the centers of the two triangular regions of the unit cell. These features are in excellent agreement with the STM observations in Figure 2b, verifying that the model of the (3 × 3) germanene/(√19 × √19) Pt(111) superstructure fundamentally resembles what we observed in our experiments. The relaxed model and the simulated STM image here provide a clear picture of the germanium arrangements in the adlayer observed in the actual STM images. The germanium atoms at the top sites of the underlying Pt atoms (the yellow spheres in Figure 3a) correspond to the bright protrusions exhibited in the STM image (Figure 2b). Furthermore, in the model, only one of the six germanium atoms in the honeycomb has a higher position, which differs from the theoretical models of a free-standing germanene sheet, wherein half of the germanium atoms have higher positions than the other half.[8] This suggests a substrate-induced buckled conformation of the germanene adlayer.

Although the germanene layer has a buckled structure with an undulation, it is a continuous layer rather than an accumulation of fragments with several germanium atoms, according to the analysis of the electron localization function (ELF).[20,21] The ELF shows the charge localization between individual atoms, allowing us to directly appraise the chemical interaction between atoms. **Figure 4**a shows the top view of the overall ELF within the germanene layer with an ELF value of 0.5. Here, we see that chemical interaction exists between each pair of germanium atoms, showing the continuity of the germanene layer. This means the germanium atoms are well bonded to each other in the germanene sheet. In order to identify the bonding characteristics within each germanium pair clearly, the ELFs along the cross-section of each Ge–Ge pair (annotated in Figure 4a) are displayed in Figure 4b–f. The ELF values are shown by the color scheme, where red represents the electrons that are highly localized and blue signifies the electrons with almost no localization. It is clearly seen that electrons are localized to a large degree at the Ge–Ge pair containing a top-most Ge atom (the magnitudes of the ELF values are in the range of ~0.75–0.84, as shown in Figure 4b,c), identifying a covalent bond between germanium atoms. The Ge–Ge pair (Figure 4f) with the largest atomic distance has a slightly lower density of electrons localized in its intermediate location (ELF value is about 0.53). In conclusion, the ELFs presented here provide evidence that a covalent interaction exists between the members of each Ge–Ge pair. For comparison, the cross-section of the ELF between the germanium atom at the hexagonally close-packed (hcp) site and its nearest Pt atom is shown in Figure 4g. The distance between such a Ge–Pt pair is the shortest one, and this is the position with the strongest interaction between the germanene layer and the substrate. However, the ELF value in this case is only 0.29, much smaller than the ELF values of any of the germanium pairs. ELF values of less than 0.5 correspond to an absence of pairing between electrons. Therefore, it can be concluded that the interaction between germanium and the underlying platinum is mainly of an electrostatic origin. This interaction is not strong enough to affect the formation of Ge–Ge bonds and the extension of the germanium sheet. The above-mentioned evidence demonstrates that a 2D continuous germanium layer – germanene – was indeed successfully fabricated on Pt(111).

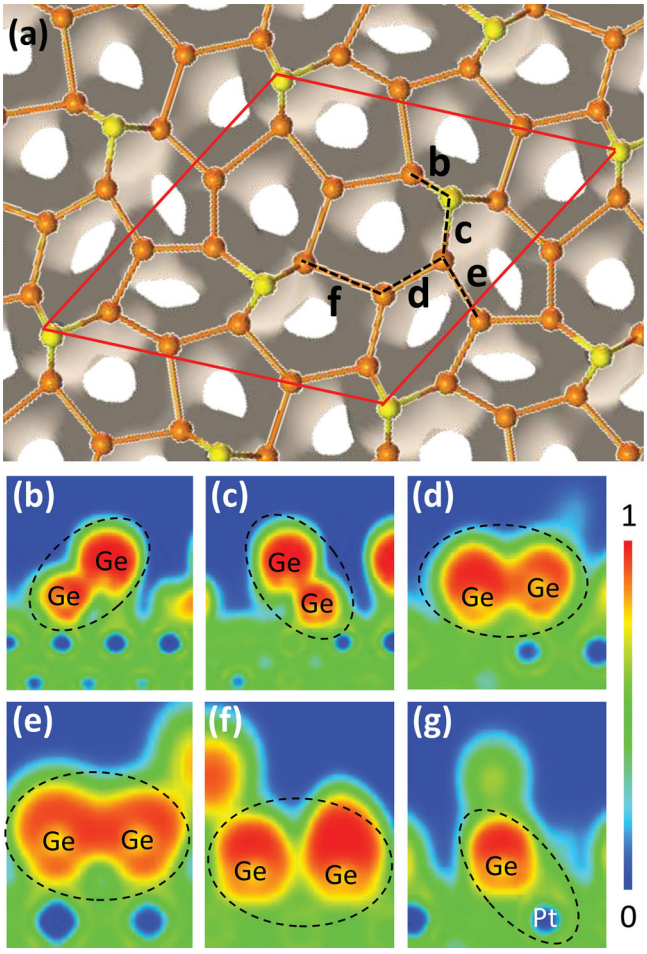

Figure 4. a) Top view of the overall electron localization function (ELF) of the relaxed model with an ELF value of 0.5, showing continuity of the germanene layer. Yellow and brown spheres represents Ge atoms, with the yellow spheres indicating the protruding Ge atoms. b–f) The ELFs of the cross-sections between the germanium pairs indicated in (a), showing the covalent interaction existing between each pair of germanium atoms. The pairs are depicted by the dashed ovals. g) The ELF of the cross-section between one germanium atom and its nearest Pt neighbor. The ELF value here is in the range of the green-blue region (about 0.29), indicating an electrostatic interaction. The color scale for (b)–(g) is shown on the right.

It is worth noting, however, that a Ge–Pt substitutional surface alloy has been claimed previously by Ho et al.[22] They annealed their sample at 900–1200 K to form a Ge–Pt surface alloy, aiming to obtain a longer catalyst lifetime. In their STM images, only four bright protrusions appear, located at the corners of each ($\sqrt{19} \times \sqrt{19}$) supercell. It is obvious that their images show fewer features per unit cell than our high-resolution STM image (Figure 2b). In their model, there is only one Ge atom within each ($\sqrt{19} \times \sqrt{19}$) supercell. This simple model is not suitable for our case, according to our theoretical simulations and experimental observations (see details in the Supporting Information). We verified that the ($\sqrt{19} \times \sqrt{19}$) superstructure in our case originates not from Ge–Pt chemical contrast but instead from the charge density of state of the buckled germanene layer supported on Pt(111).

In summary, germanene has been successfully fabricated on Pt(111). It has a ($\sqrt{19} \times \sqrt{19}$) superstructure related to the substrate lattice, as demonstrated by low-energy electron diffraction and scanning tunneling microscopy. Calculations based on first principles reveal that such a superstructure coincides with the (3×3) superlattice of a buckled germanene sheet. Furthermore, the calculated electron localization function shows that adjacent germanium atoms directly bind to each other, certifying the formation of a continuous 2D germanene sheet on the Pt(111) surface. This work provides a method of producing high-quality germanene on solid surfaces so as to explore its physical properties and potential applications in future functional nanodevices.

Experimental Section

Experiments were performed in an ultra-high vacuum (UHV) system with a base pressure of about 2×10^{-10} mbar. The Pt(111) substrate was cleaned by several cycles of sputtering and annealing until it yielded distinct Pt(1×1) diffraction spots in the LEED pattern and clean surface terraces in the STM images. The germanium was deposited on Pt(111) at room temperature under UHV conditions from a germanium rod mounted in an electron-beam evaporator. After deposition, the sample was annealed at a temperature range of 600–750 K for 30 min. We annealed the samples at temperatures below 800 K, for the sake of excluding the formation of a Ge–Pt surface alloy. We used LEED to identify the superstructures macroscopically. STM was then employed to image the surface at the atomic level.

Computation: Our DFT-based first-principle calculations were performed using the Vienna ab initio simulation package (VASP).[23,24] The projector augmented wave (PAW) potentials were used to describe the core electrons, and the local density approximation (LDA) was used for exchange and correlation.[25] The periodic slab models included four layers of Pt, one layer of germanium, and a vacuum layer of 15 Å. All atoms were fully relaxed except for the bottom two substrate layers until the net force on every atom was less than 0.01 eV/Å. The energy cutoff of the plane-wave basis sets was 400 eV, and the K-points sampling was $3 \times 3 \times 1$, generated automatically with the origin at the Γ-point.

Supporting Information

Supporting Information is available from the Wiley Online Library or from the author.

Acknowledgments

The authors gratefully acknowledge the financial support from the National Key Basic Research Program of China (Nos. 2013CBA01600 and 2011CB932700), the NSFC (Nos. 61222112, 11004219 and 11334006), and CAS in China.

Received: February 26, 2014
Revised: April 14, 2014
Published online: May 20, 2014

[1] Y. B. Zhang, Y. W. Tan, H. L. Stormer, P. Kim, *Nature* **2005**, *438*, 201.
[2] K. S. Novoselov, A. K. Geim, S. V. Morozov, D. Jiang, M. I. Katsnelson, I. V. Grigorieva, S. V. Dubonos, A. A. Firsov, *Nature* **2005**, *438*, 197.
[3] A. H. Castro Neto, F. Guinea, N. M. R. Peres, K. S. Novoselov, A. K. Geim, *Rev. Mod. Phys.* **2009**, *81*, 109.

[4] K. S. Novoselov, V. I. Fal'ko, L. Colombo, P. R. Gellert, M. G. Schwab, K. Kim, *Nature* **2012**, *490*, 192.
[5] L. A. Ponomarenko, R. V. Gorbachev, G. L. Yu, D. C. Elias, R. Jalil, A. A. Patel, A. Mishchenko, A. S. Mayorov, C. R. Woods, J. R. Wallbank, M. Mucha-Kruczynski, B. A. Piot, M. Potemski, I. V. Grigorieva, K. S. Novoselov, F. Guinea, V. I. Fal'ko, A. K. Geim, *Nature* **2013**, *497*, 594.
[6] C. R. Dean, L. Wang, P. Maher, C. Forsythe, F. Ghahari, Y. Gao, J. Katoch, M. Ishigami, P. Moon, M. Koshino, T. Taniguchi, K. Watanabe, K. L. Shepard, J. Hone, P. Kim, *Nature* **2013**, *497*, 598.
[7] Y. Pan, H. Zhang, D. Shi, J. Sun, S. Du, F. Liu, H.-J. Gao, *Adv. Mater.* **2009**, *21*, 2777.
[8] S. Cahangirov, M. Topsakal, E. Aktürk, H. Şahin, S. Ciraci, *Phys. Rev. Lett.* **2009**, *102*, 236804.
[9] P. Vogt, P. De Padova, C. Quaresima, J. Avila, E. Frantzeskakis, M. C. Asensio, A. Resta, B. Ealet, G. Le Lay, *Phys. Rev. Lett.* **2012**, *108*, 155501.
[10] B. Feng, Z. Ding, S. Meng, Y. Yao, X. He, P. Cheng, L. Chen, K. Wu, *Nano Lett.* **2012**, *12*, 3507.
[11] A. Fleurence, R. Friedlein, T. Ozaki, H. Kawai, Y. Wang, Y. Yamada-Takamura, *Phys. Rev. Lett.* **2012**, *108*, 245501.
[12] L. Meng, Y. Wang, L. Zhang, S. Du, R. Wu, L. Li, Y. Zhang, G. Li, H. Zhou, W. A. Hofer, H.-J. Gao, *Nano Lett.* **2013**, *13*, 685.
[13] C.-C. Liu, W. Feng, Y. Yao, *Phys. Rev. Lett.* **2011**, *107*, 076802.
[14] G. Baskaran, *arXiv:1309.2242* **2013**.
[15] M. Gao, Y. Pan, C. Zhang, H. Hu, R. Yang, H. Lu, J. Cai, S. Du, F. Liu, H.-J. Gao, *Appl. Phys. Lett.* **2010**, *96*, 053109.
[16] M. Gao, Y. Pan, L. Huang, H. Hu, L. Z. Zhang, H. M. Guo, S. X. Du, H.-J. Gao, *Appl. Phys. Lett.* **2011**, *98*, 033101.
[17] R. Addou, A. Dahal, M. Batzill, *Nat. Nanotechnol.* **2013**, *8*, 41.
[18] J. Gao, J. Zhao, *Sci. Rep.* **2012**, *2*, 861.
[19] J. Tersoff, D. R. Hamann, *Phys. Rev. B* **1985**, *31*, 805.
[20] A. D. Becke, K. E. Edgecombe, *J. Chem. Phys.* **1990**, *92*, 5397.
[21] A. Savin, O. Jepsen, J. Flad, O. K. Andersen, H. Preuss, H. G. Vonschnering, *Angew. Chem. Int. Ed. Engl.* **1992**, *31*, 187.
[22] C.-S. Ho, S. Banerjee, M. Batzill, D. E. Beck, B. E. Koel, *Surf. Sci.* **2009**, *603*, 1161.
[23] D. Vanderbilt, *Phys. Rev. B* **1990**, *41*, 7892.
[24] G. Kresse, J. Furthmuller, *Phys. Rev. B* **1996**, *54*, 11169.
[25] J. P. Perdew, K. Burke, M. Ernzerhof, *Phys. Rev. Lett.* **1996**, *77*, 3865.